Cell Reports, Volume *22*

Supplemental Information

Balance Control Mediated by Vestibular Circuits Directing Limb Extension or Antagonist Muscle Co-activation

Andrew J. Murray, Katherine Croce, Timothy Belton, Turgay Akay, and Thomas M. Jessell

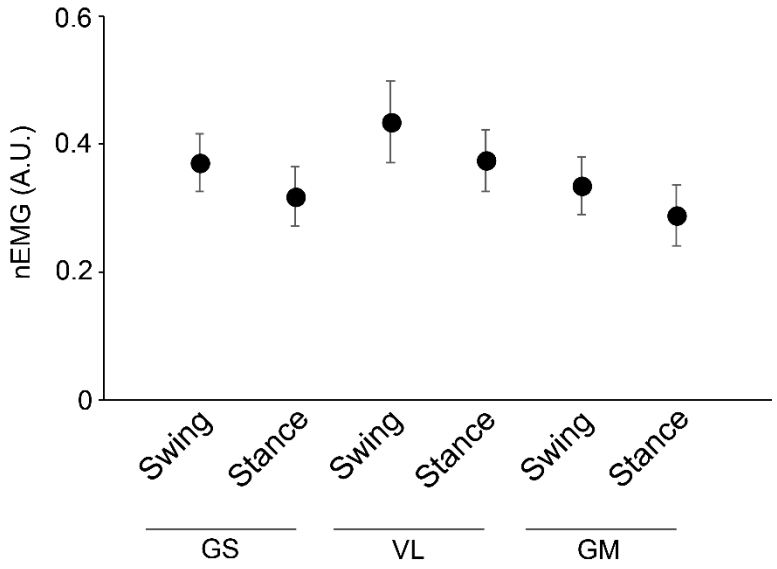

Supplementary Figure 1. Relates to Figure 1. Effect of swing or stance phase of step cycle on early phase EMG response after balance beam perturbation.

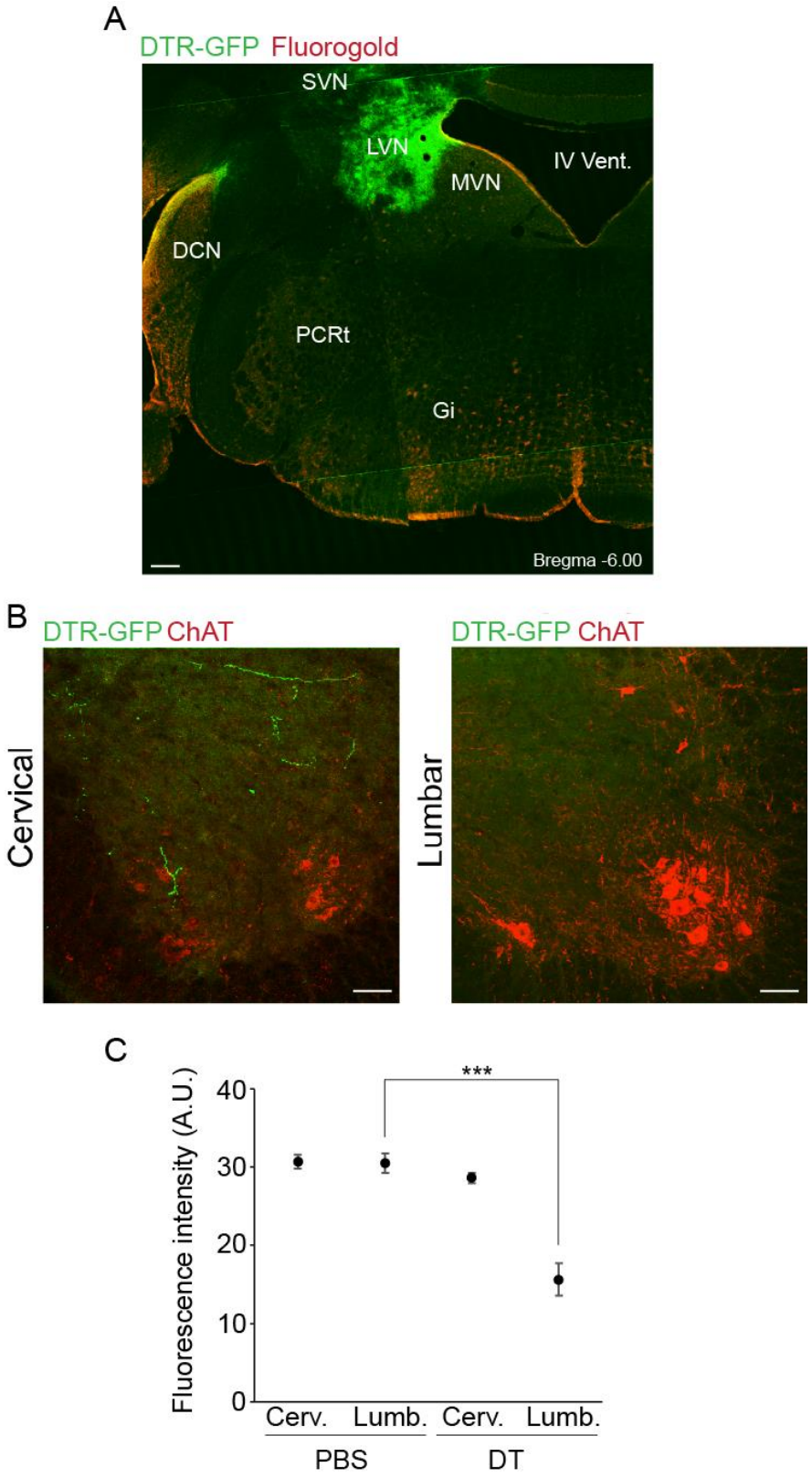

Supplementary Figure 2. Relates to Figure 2. Specificity of AAV-DTR ablation. (A) Coronal brain section showing injection site of AAV-DTR-GFP. This is a widefield view of the LVN injection site from Figure 2B, C. Image is a composite of several tiles automatically stitched together during acquisition. (B) Vestibulospinal axons are found in the cervical spinal cord (left) but not present in the lumbar spinal cord after DT injection. (C) Quantification of GFP fluorescence intensity in sections of cervical (cerv.) or lumbar (lumb.) spinal cord after DTR-GFP injection in the LVN and either PBS (control) or diphtheria toxin (DT) injection into the lumbar spinal cord. ***$p<0.001$. Data presented as mean ±S.E.M. Scale bars in A = 100 µm, B = 50 µm.

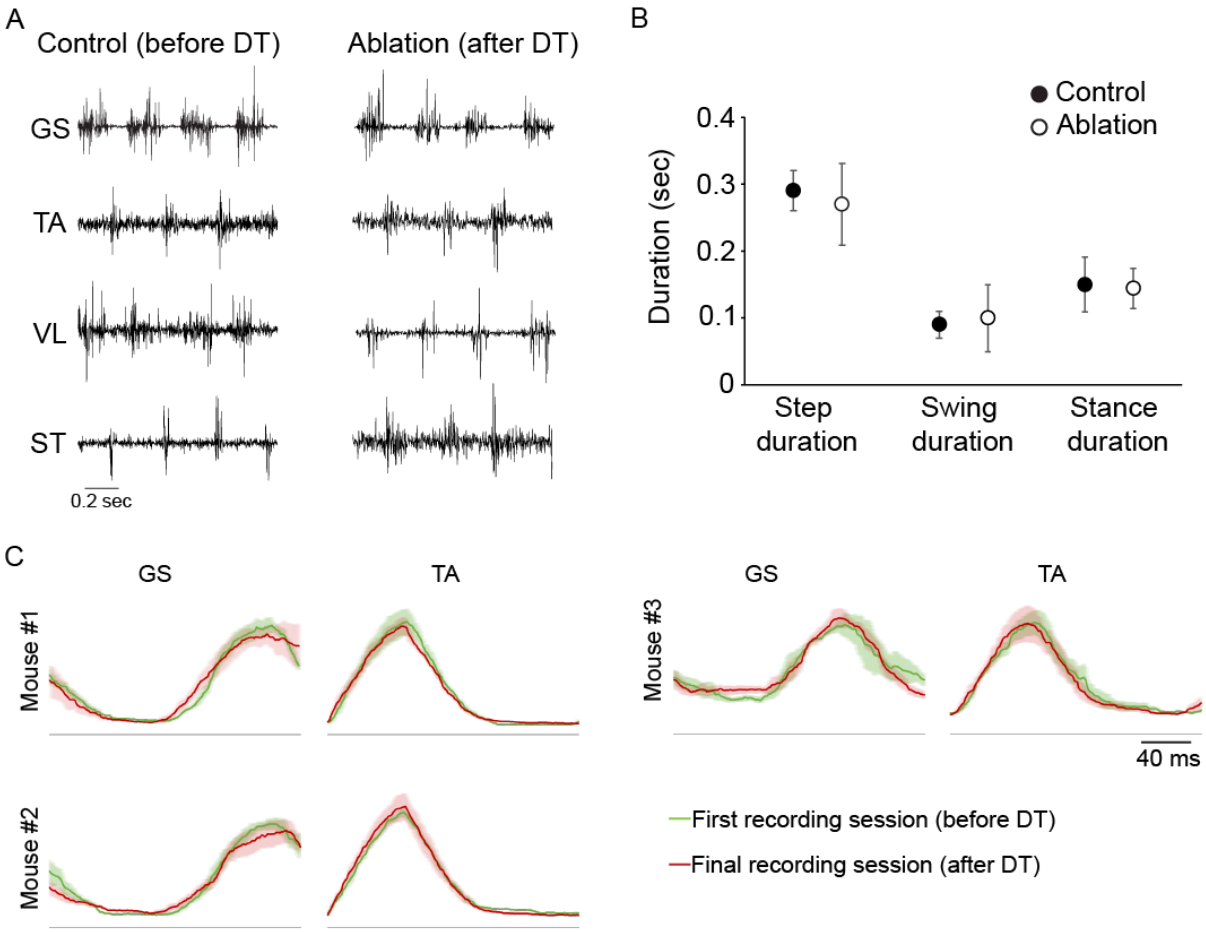

Supplementary Figure 3. Relates to Figure 2. Treadmill walking and long-term stability of EMG recordings after ablation of lumbar projecting LVN neurons. (A) Example EMG traces in the GS, TA, VL and ST muscles. (B) Analysis of step, swing and stance durations during treadmill walking at 0.2 m/s. (C) Mean rectified EMG signals (±standard deviation) from the gastrocnemius (GS) and tibialis anterior (TA) muscles in individual step cycles as animals walk on a treadmill at 0.3 m/s. Green trace shows EMG from the first recording session after implantation, red trace from final recording session after diphtheria toxin injection. Data presented as mean ±S.D.

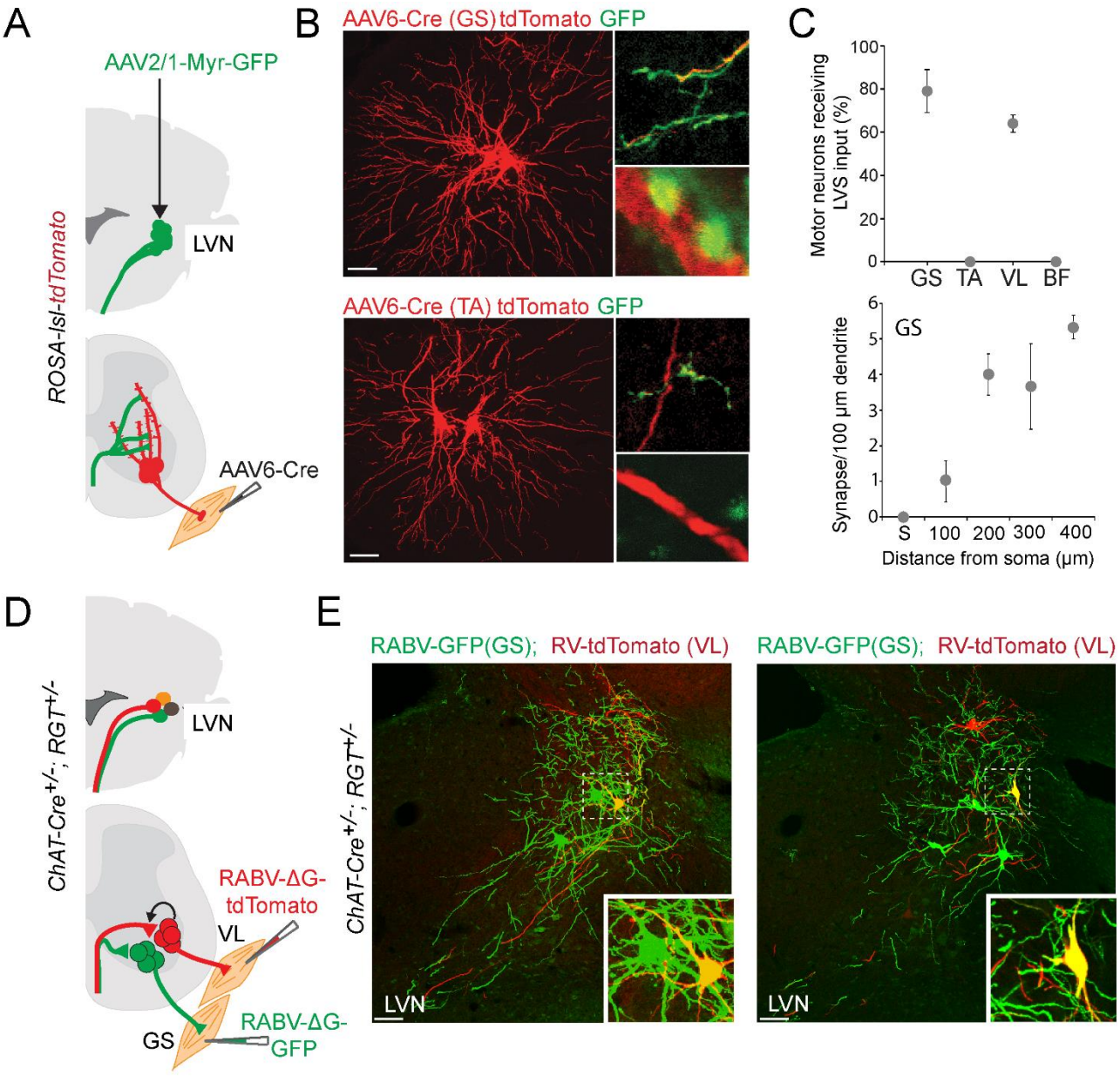

Supplementary Figure 4. Relates to Figures 3 and 4. Specificity of LVN innervation of extensor motor neurons. (A) Experimental strategy for orthograde tracing from the LVN to lumbar spinal cord. (B) Example GS or TA motor neuron dendritic arbor and putative LVN synapses. Synaptophysin labeling used in quantification omitted for clarity. (C) Quantitation of LVN synapses onto extensor or flexor motor neurons. (D) Experimental design for dual-color labelling of LVN neurons innervating the GS and VL motor pools. (E) Images of the LVN showing yellow neurons that innervate both GS and VL motor neurons. Scale bar in B = 30 µm, E = 50 µm.

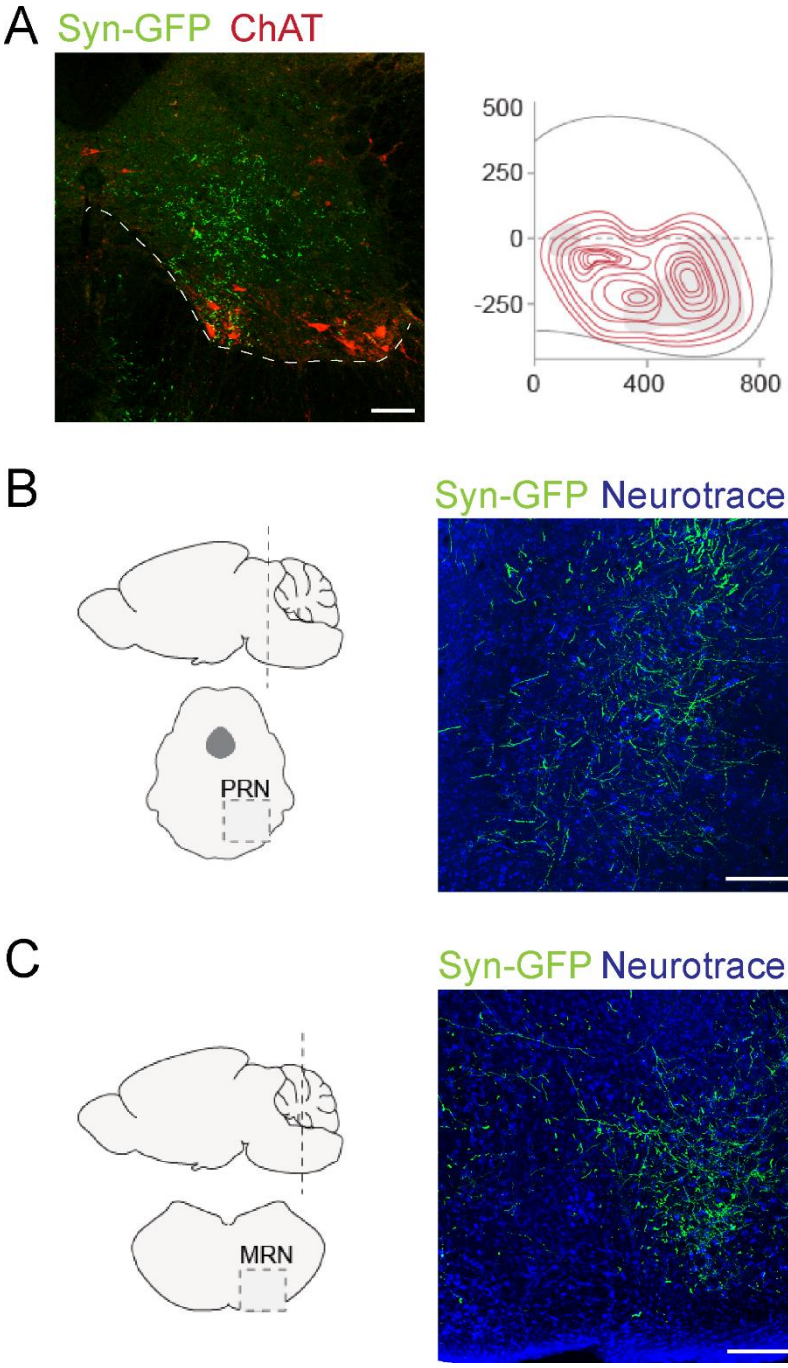

Supplementary Figure 5. Relates to Figures 4 and 5. Assaying LVN projections with injection of AAV encoding a GFP-tagged synaptophysin. (A) Synapses in the lumbar spinal cord cover the majority of the ventral portion, as revealed by plot showing position of synapses in the ventral spinal cord (right). (B) Synapses were also found in the pontine reticular nucleus and (C) the medullary reticular nucleus. Scale bar in A = 50 µm, B and C = 200 µm.

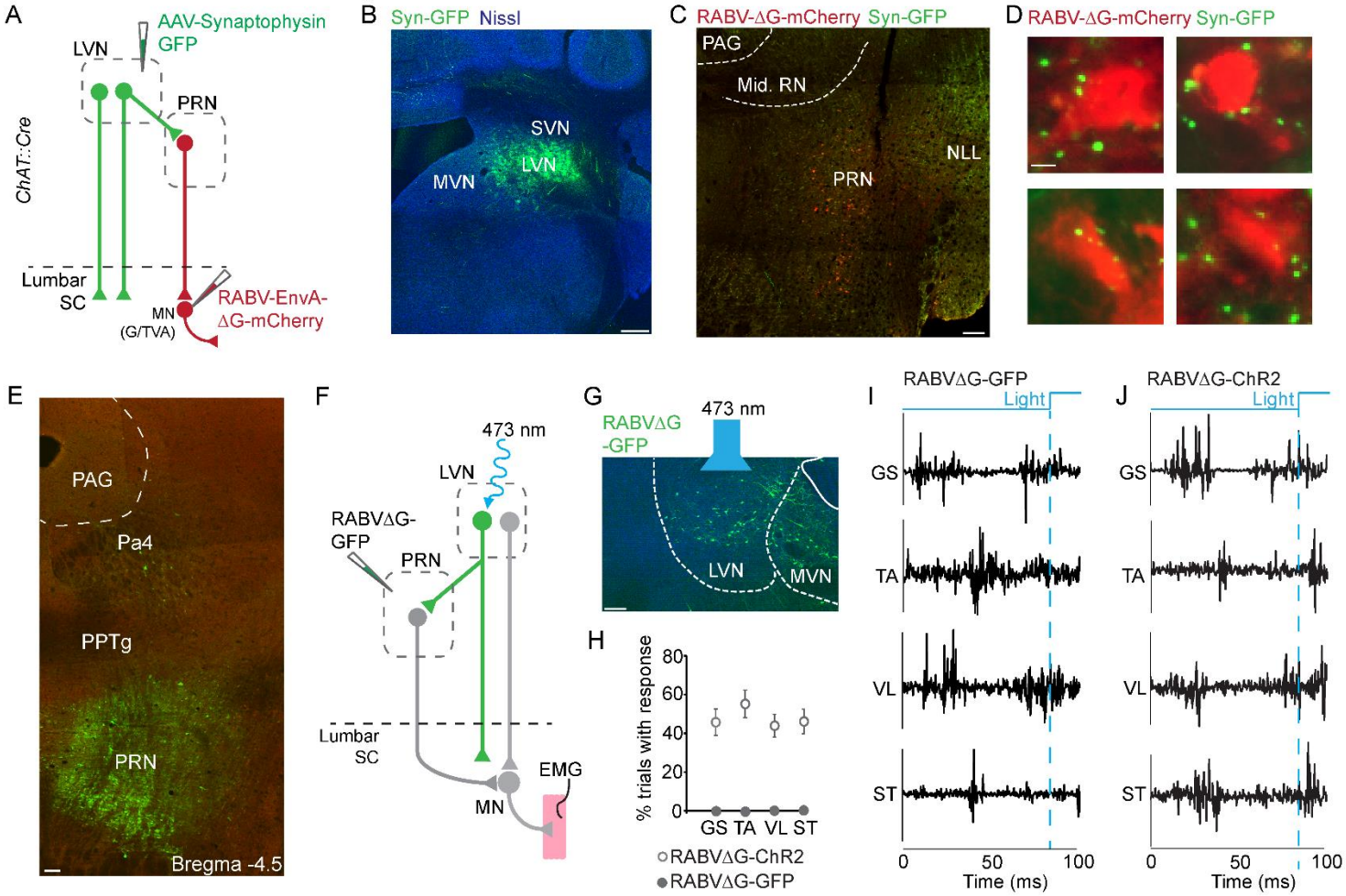

Supplementary Figure 6. Relates to Figures 5, 6 and 7. Circuit mapping of the LVN-PRN connection. (A) Experimental scheme to identify PRN neurons postsynaptic to the LVN and presynaptic to spinal motor neurons. (B) Injection site of AAV-synaptophysin-GFP. (C) mCherry-positive neurons in the PRN labelled by monosynaptic transfer from lumbar spinal motor neurons. (D) Images of PRN premotor neurons receiving synaptic contacts from the LVN. (E) Coronal brain section showing injection site of AAV-DTR-GFP into the PRN. Experimental details are for main text Figure 7A,B. (F) Experimental scheme for control optogenetic experiments using GFP in place of ChR2. (G) Retrogradely infected neurons expressing GFP in the vestibular nuclei with approximate position of fiber optic cannula indicated. (H) Percentage of walking trials that resulted in EMG signal concomitant with light activation in ChR2 expressing animals (open circles; data also shown in Figure 6E) and in separate cohort (n=3) expressing GFP. (I) EMG recordings in the GS, TA, VL and ST muscle as GFP-expressing animals walk on the balance beam. (J) Data from Figure 6C shown for comparison to (I), optogenetic stimulation of animals expressing ChR2 as they walk on the balance beam.

B, C and E are a composite of several tiles automatically stitched together during acquisition. SVN = superior vestibular nucleus; MVN = medial vestibular nucleus; LVN = lateral vestibular nucleus; PAG -periaqueductal gray; Pa4 – Parvotrochlear nucleus; PPTg – Pedunculopointine reticular nucleus; PRN- pontine reticular nucleus; Mid. RN – Midbrain reticular nucleus; NLL – Nucleus of the lateral leminiscus; PRN – Pontine reticular nucleus. Syn-GFP - Synaptophysin-GFP. Scale bars in B and C = 150 µm, D = 10 µm, E = 200 µm, G= 100 µm.

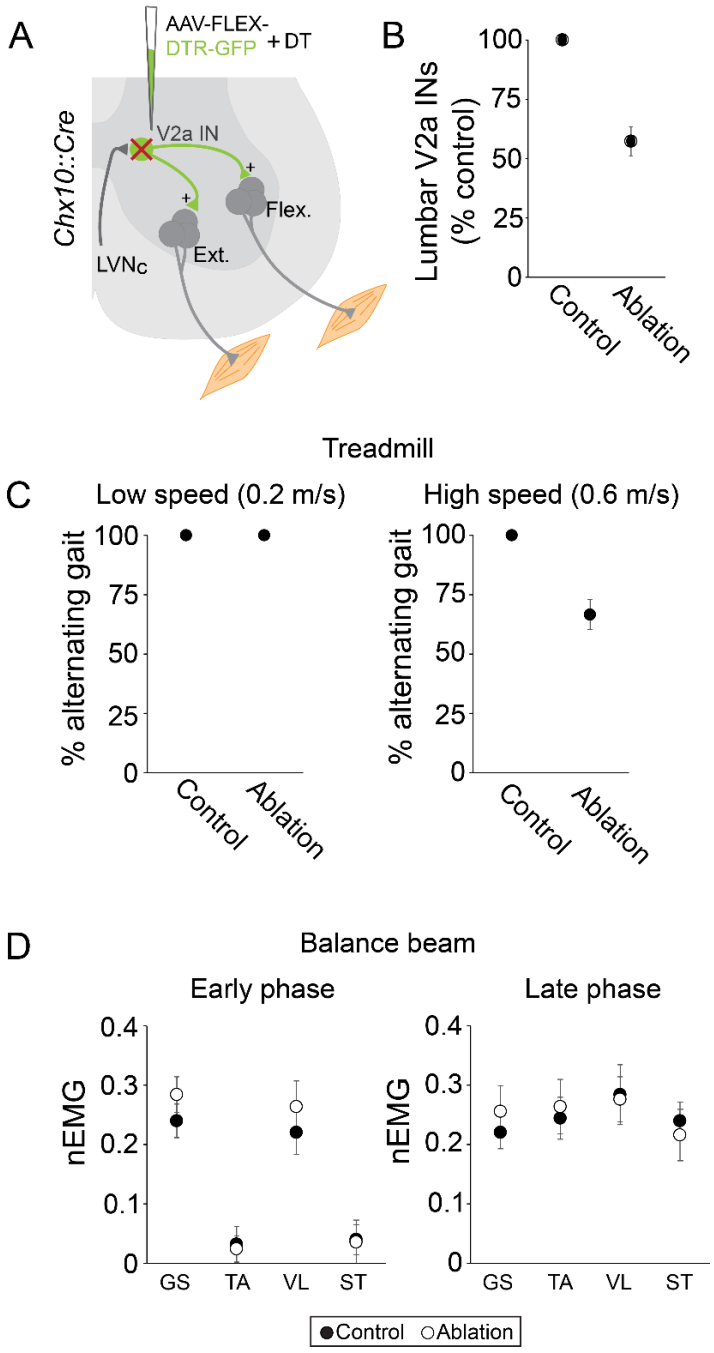

Supplementary Figure 7. Relates to Figures 6 and 7. Ablation of lumbar spinal cord V2a interneurons. (A) Experimental strategy for V2a ablation. (B) Quantification of V2a ablation. (C) Alternating gait on the treadmill at high and low speeds. (D) Normalized EMG quantification of early and late phase EMG responses with balance beam perturbation before and after V2a ablation.

Supplemental experimental procedures

Resource table

Antibodies		
Rabbit anti GFP	ThermoFisher	A-11122
Goat anti GFP	Abcam	Ab6673
Rabbit Anti mCherry	Abcam	Ab167453
Rabbit anti choline acetyl transferase	Jessell Laboratory	N/A
Rabbit anti synaptophysin	Abcam	Ab32127
Rabbit anti fluorogold	EMD Millipore	AB153
Guinea Pig anti fluorogold	Protos Biotech	NM-101 FluGP
Chemicals, peptides and recombinant proteins		
Fluorogold	Sigma	39286
Cholera toxin beta subunit – Alexa 647 conjugate	ThermoFisher	C34778
Cholera toxin beta subunit – Alexa 647 conjugate	ThermoFisher	C34776
Diphtheria Toxin	Sigma	D0564
Mouse Lines		
ChAT::Cre	Rossi et al., 2011	RRID: IMSR_JAX:006410
RGT	Takatoh et al., 2013	Jackson Laboratories: 024708
Chx10::Cre	Azim et al., 2014/Jessell Laboratory	N/A
Recombinant DNA		
pAM-fDIO-Synaptophysin-GFP	This paper/ Submitted to Addgene	N/A
pAM-Synaptophysin-GFP	This paper/ Submitted to Addgene	N/A
pAM-CAGGS-FLEX-H2B-GFP-P2A-N2c(G)	Reardon et al., 2016	Addgene: 73475
RABV CVS-N2c(deltaG)-dsRed	Reardon et al., 2016	Addgene: 73460
RABV CVS-N2c(deltaG)-hChR2-YFP	Reardon et al., 2016	Addgene: 73465
RabV CVS-N2c(deltaG)-mCherry-P2A-FlpO	Reardon et al., 2016	Addgene: 73471
pAAV-EF1a-FLEX-TVA-mCherry	Watabe-Uchida et al., 2012	Addgene: 38044
Cell Lines		
Neuro2A-N2cG	Reardon et al., 2016/Available from corresponding authors	N/A
Neuro2A-EnvA	Reardon et al., 2016/Available from corresponding authors	N/A
Physiology and optogenetics		
EMG Electrodes (see also Akay, 2014)		
Implantation wire	A-M Systems	793200
Connectors	Digi-Key	SAM1153-12-ND
Amplifier	University of Cologne	MA102S
Pre amplifier	University of Cologne	MA103S
Analogue-digital converter	Cambridge Electronic Design	CED1401
Optogenetics		
Mono fiber optic cannula	Doric Lenses	MFC_400/430
Mono Fiberoptic Patchcord	Doric Lenses	MFP_200/230/900-0.48_1.8m
473 nm diode lazer	Crysta laser	473 nm Blue Laser

Behavior		
Treadmill	University of Cologne	802
Piezomotor Controller / Driver	Physik Instrumente	C-867.160
PILine Precision Rotation Stage	Physik Instrumente	M-660.45
Software		
Spike 2	Cambridge Electronic Design	CED Spike 2
R	R-Project	R-Project.org
PI MikroMove	Physik Instrumente	PI MikroMove
Image J	NIH	imagej.nih.gov/ij/

Contact for reagent and resource sharing

Further information and request for resources and reagents should be directed to and will be fulfilled by either Thomas Jessell (tmj1@columbia.edu) or Andrew Murray (a.murray@ucl.ac.uk).

Method details

Balance Beam Assay

The balance beam assay was carried out on a custom built behavioral setup consisting of a 5 mm wide metal beam with perturbations driven by a piezo rotation stage (Physik Instrumente). Naive mice started with two days of "practice" sessions (5-10 runs along the beam per day) where they are allowed to traverse the beam freely without a perturbation in order to familiarize themselves with the apparatus. On the three subsequent days perturbations were introduced in ~1 of 3 trials. Approximately equal numbers of perturbations were given to the left and right to minimize habituation. Typically, after one to two days of perturbations behavioral and EMG responses become stereotyped. The results reflect trials where the balance beam was moved to the left (with EMG electrodes implanted in the right hindlimb) but behavioral trials consisted of both rightward and leftward perturbations to minimize habituation. Behavioral analysis typically started one week after beginning this training.

Additionally, the point on the beam at which the mouse received a perturbation was randomized. Daily behavioral trials consisted of 20-30 beam runs, consisting of approximately one third leftward perturbations, one third rightward perturbations and one third without a perturbation. We carried out between three and six behavioral sessions per animal before experimental manipulation (i.e. diphtheria toxin injection) and between three and five sessions after manipulation (starting at 10 days post diphtheria toxin injection). Sessions in which the animal was not actively moving as it received a perturbation (assessed via the EMG trace and high speed video recordings) were not included in the analysis.

Viral Vectors

To ablate LVN or PRN neurons projecting to the lumbar spinal cord we used an adeno-associated virus (AAV) encoding the diphtheria toxin receptor (Azim et al., 2014). Two weeks after stereotaxic injection of AAV we injected 10 nl of 2 ng/µl mg/ml diphtheria toxin at lumbar level 3.

To selectively express a GFP-tagged synaptophysin in LVN_E neurons we generated a FLP-recombinase dependent AAV (pAAV-fDIO-Syn-GFP). The eYFP gene was removed from pAAV-EF1α-fDIO-eYFP (Addgene plasmid 55641; a gift of Karl Deisseroth) via AscI and NheI restriction sites. The coding region for a synaptophysin-GFP fusion protein was inserted inverted between frt sites.

AAV vectors were produced as described previously (McClure et al., 2011). Briefly, for the AAV plasmid, AAV RepCap sequences for AAV1 and AAV2 and the AAV helper plasmid pFdelta6 was transfected into Hek293 cells using calcium phosphate. After three days the cells were harvested and lysed, and viral

particles were purified using a HiTrap Heparin cartridge (Millipore) and concentrated with a centrifugal filter unit (Amicon Ultra).

SAD-B19ΔG rabies virus vectors were used for monosynaptic tracing from extensor motor neurons via complementation with the B19 glycoprotein from the RGT mouse line were used to trace monosynaptic inputs to motor neurons. SAD-B19ΔG rabies virus was produced as described previously (Osakada and Callaway, 2013; Zampieri et al., 2014). CVS-N2cΔG rabies virus was used for all other experiments, including expression of channelrhodopsin in LVN_E and LVN_C neurons and flp-mediated recombination of pAAV-fDIO-Syn-GFP. Production of CVS-N2cΔG was carried out as described previously (Reardon et al., 2016).

Mouse Surgery

EMG Implant and Recordings

Bipolar EMG recording electrodes were implanted into combinations of GS, TA, VL, ST, GM and BF muscles. Each animal received implants into either four or six muscles, with extensor-flexor antagonists implanted in the same animal. Surgeries were carried out as described previously (Akay et al., 2014). Briefly, the dorsal neck and right hind-limb was shaved. Incisions were made at the neck and at the hind-limb above the muscles to be implanted. Custom made bipolar electrodes were led under the skin from the neck incision to the leg incisions and implanted into appropriate muscles. The incisions were closed with sutures and the mice were left in their cages for recovery for at least 4 days before recordings began.

Following recovery, implanted EMG electrodes were attached to an amplifier (model: MA 102; custom built in the workshop of the Zoological Institute, University of Cologne) via the headpiece connector at their neck (Akay et al., 2014). Behavioral testing was recorded via a high speed camera (120 fps for balance beam; 240 fps for treadmill running) using custom built reflectors placed at hind-limb joints (Akay et al., 2014) for later analysis. Kinematic parameters were calculated using MaxTraq 2D software (Innovision Systems).

Stereotaxic Surgery

Stereotaxic injection into the LVN was carried out as described previously (Murray et al., 2015). Briefly, animals were anesthetized with 3% isofluorane in oxygen and maintained on 1-2% isofluorane in oxygen. The scalp was cleaned and a horizontal incision made on the top of the skull. A dental drill was used to make a small burr hole at the appropriate position on the skull. Stereotaxic injection coordinates relative to Bregma for the LVN were anterior/posterior -6.05 mm; lateral 1.38 mm. 100 nl of solution was injected at each depth of -4.5 mm, -4.4 mm and -4.3 mm using a Nanoject II (Drummond). The burr hole was filled with sterile bone wax and the skin closed with VetBond. Animals were allowed to recover for at least 48 hours before behavioral testing.

Spinal Cord Injections

Surgery was identical for injection of diphtheria toxin, fluorogold (20 nl of 2% solution in saline), rabies virus (300 nl of EnvA-pseudotyped rabies virus) or AAV2/1 (200 nl) into the lumbar spinal cord. Animals were anaesthetized with 3% isofluorane in oxygen and maintained in 1-2% isoflourane for the duration of the surgery. The fur along the back rostral to the hindlimbs was shaved, the area cleaned and an approximate

3 cm incision was made above the lumbar spinal cord. A small domain of axial muscle was removed and a ~0.5 mm slit was cut in the vertebrae. Injections were carried out at -1.00 mm from the dorsal surface of the spinal cord to target the ventral horn. The incision was closed with sutures and animals were allowed to recover for at least 48 hours before any behavioral testing.

Ablation of lumbar spinal projecting LVN neurons

AAV-DTR-GFP was injected into the LVN (see Stereotaxic Surgery) and allowed to express for at least three weeks. During this time EMG recording electrodes were also implanted into the hindlimb. Control recordings were made from at least three separate sessions with each session including treadmill and balance beam trials. Animals then underwent a lumbar spinal injection of diphtheria toxin (10 nl of a 2 ng/ul DT solution) directly into the spinal cord at an angle of 10° and depth of 1.00 mm from the cord surface. Animals were allowed to recover for two weeks before continuation of recordings. After the final set of EMG recordings the animals received a spinal injection of 2% fluorogold (50 nl in PBS) to label descending neurons. The number of fluorogold positive neurons in the LVN was used to quantify the effectiveness of the ablation.

Muscle Inoculation of Rabies Virus

For rabies tracing experiments, *ChAT-CRE::RGT* animals at postnatal day 4 were anesthetized with 4% isofluorane in oxygen and 2 µl of RVΔG-GFP-EnvA or RVΔG-GFP was inoculated with a glass capillary either into the GS, TA, VL or BF muscle visualize for monosynaptic inputs to motor neurons. Animals were sacrificed 6 days later by transcardial perfusion with phosphate buffered saline followed by 4% paraformaldehyde in phosphate buffer.

Histology

For histological analysis, mice were transcardially perfused with phosphate buffered saline (PBS), then 4% paraformaldehyde (PFA) in phosphate buffer. Brains and spinal cords were postfixed in 4% PFA for 2 hours at 4°C, washed in PBS and cryoprotected in 30% sucrose in PBS for 24 hours. The tissue was cut into blocks and frozen on optimum cutting temperature (OCT) compound. 50 µm sections were cut on a Leica cryostat. Where required immunostainng was carried out as previously described (Zampieri et al., 2014). To aid histological identification of brain regions and the location of viral injections sections were counterstained with the fluorescent nissl stain, Neurotrace (Life Technologies). Imaging was carried out on a on a Zeiss LSM 510 or 710 confocal. Brain and spinal cord sections were tile scanned and automatically stitched together with Zeiss Zen software.

Optogenetic Activation of LVN_E or LVN_C neurons

For optogenetic activation of LVN_E neurons, neonatal *ChAT::Cre* mice were injected into the GS muscle with a combination of cre-conditional AAVs encoding the TVA receptor and the CVS-N2c glycoprotein. Two to Three weeks later EnvA-pseudotyped CVS-N2c rabies virus encoding ChR2 (Reardon et al., 2016) was injected into the lumbar spinal cord. A fiber optic cannula comprised of a zirconia ferrule housing an optical fibre (200 µm core diameter, length 6.1 mm; Doric Lenses) was inserted into the LVN (from Bregma: anterior-posterior 6.05 mm; lateral 1.35 mm; depth 4.5 mm). The ferrule was secured to the back of the skull using dental cement as described (Azim et al., 2014). Optical stimulation was carried out between 12 and 16 days after

rabies virus injection (Reardon et al., 2016) while animals were walking on a treadmill or traversing the balance beam. Light was delivered using a mono fibre-optic patch cord connected to the ferrule via a zirconia sleeve (Doric Lenses). A 473 nm diode laser (CrystaLaser) and Cambridge Electronic Designs 1401 analogue-digital converter was used to generate pulses of light via a TTL pulse (15 ms pulse width, 20 Hz, ~10 mW). Laser strength was measured at the end of the ferrule tip using a light power meter (Thor Labs) before implantation.

Optical activation of LVNc neurons was carried out as above except that glycoprotein coated CVS-N2c rabies virus encoding ChR2 was injected into the PRN to directly infect LVN terminals. Optogenic experiments were carried out between 12 and 16 days after rabies virus injection.

Supplementary References

Akay, T., 2014. Long-term measurement of muscle denervation and locomotor behavior in individual wild-type and ALS model mice. J. Neurophysiol. 111, 694–703.

McClure, C., Cole, K.L.H., Wulff, P., Klugmann, M., Murray, A.J., 2011. Production and titering of recombinant adeno-associated viral vectors. J. Vis. Exp. 57. e3348.

Murray AJ, Woloszynowska-Fraser MU, Ansel-Bollepalli L, Cole KL, Foggetti A, Crouch B, Riedel G, Wulff P. 2015 Parvalbumin-positive interneurons of the prefrontal cortex support working memory and cognitive flexibility. Sci Rep. 5:16778.

Watabe-Uchida M, Zhu L, Ogawa SK, Vamanrao A, Uchida N. 2012 Whole-brain mapping of direct inputs to midbrain dopamine neurons. Neuron. 74(5):858-73.

Zampieri N, Jessell TM, Murray AJ. 2014 Mapping sensory circuits by anterograde transsynaptic transfer of rabies virus. Neuron. 81(4):766-778.